Perfusion-weighted magnetic resonance imaging in the evaluation of focal neoplastic and infectious brain lesions

Perfusão por ressonância magnética na avaliação das lesões focais neoplásicas e infecciosas do encéfalo

Valdeci Hélio Floriano[1], José Roberto Lopes Ferraz-Filho[2], Antonio Ronaldo Spotti[3], Waldir Antônio Tognola[4]

Resumo

A ressonância magnética (RM) é o método de diagnóstico por imagem de escolha na avaliação encefálica, entretanto as técnicas convencionais de RM podem apresentar limitações por fornecerem somente parâmetros qualitativos ou anatômicos. Nas últimas décadas, têm surgido novas técnicas complementares de RM que fornecem parâmetros quantitativos proporcionando informações funcionais ou metabólico-bioquímicas. A perfusão é atualmente uma destas técnicas que vem se apresentando como uma importante ferramenta na neurorradiologia. O objetivo deste artigo é apresentar uma revisão sobre o papel da seqüência de perfusão por RM na avaliação das lesões focais neoplásicas e infecciosas, únicas ou múltiplas, do encéfalo. O estudo da perfusão encefálica pode ser realizado como método complementar às técnicas convencionais de RM, permitindo o acesso aos parâmetros hemodinâmicos de uma maneira não invasiva e demonstrando o grau de angiogênese das lesões sendo, portanto, útil na diferenciação entre lesões neoplásicas e infecciosas, tumor primário e metástase única e no seguimento pós-tratamento para a diferenciação entre recidiva tumoral e radionecrose, através da demonstração da presença ou ausência de hiperperfusão.

Palavras-chave: *perfusão, ressonância magnética, encéfalo, neoplasias, infecção.*

Abstract

Magnetic resonance imaging (MRI) is the gold standard method for brain assessment however the conventional MRI techniques may present limitations by only providing qualitative or anatomic parameters. Over recent decades, new complementary MRI techniques have been developed that supply quantitative parameters providing functional or metabolic-biochemical data. Perfusion-weighted imaging, one of these techniques, has become a powerful tool in neuroradiology. The goal of this article is to present a review about the role of perfusion-weighted MRI in the evaluation of solitary or multiple, neoplastic and infectious, focal brain lesions. Brain perfusion studies can be achieved as a complementary method to conventional MRI techniques to provide hemodynamic parameters using a non-invasive technique. This method demonstrates the degree of angiogenesis of lesions and is thus useful in the differentiation between neoplastic and infectious lesions, primary tumors and solitary metastases and in the post-treatment follow up to differentiate between tumoral recurrence and radionecrosis by identifying the presence or absence of hyperperfusion.

Keywords: *perfusion, magnetic resonance imaging, brain, neoplasms, infection.*

[1]MD. Radiologist, Department of Medical Imaging, and master2 s candidate Health Sciences Program of the Faculdade de Medicina de São José do Rio Preto (FAMERP), São José do Rio Preto, São Paulo, Brazil.
[2]MD, MSc. Assistant professor of Neuroradiology, Department of Medical Imaging, Faculdade de Medicina de São José do Rio Preto (FAMERP), São José do Rio Preto, São Paulo, Brazil.
[3]MD, PhD. Adjunct professor of Neurosurgery, Department of Neurological Sciences, Faculdade de Medicina de São José do Rio Preto (FAMERP), São José do Rio Preto, São Paulo, Brazil.
[4]MD, PhD. Adjunct professor of Neurology, Department of Neurological Sciences, Faculdade de Medicina de São José do Rio Preto (FAMERP), São José do Rio Preto, São Paulo, Brazil.

Faculdade de Medicina de São José do Rio Preto - FAMERP. Departamento de Imagem
Av. Brigadeiro Faria Lima, 5544 São José do Rio Preto, São Paulo, Brasil CEP 15090-000 Tel. (+ 55 17) 3201-5743

Introduction

Magnetic resonance imaging (MRI) is the gold standard method in brain assessment. However, the conventional MRI techniques may present limitations by only providing qualitative or anatomic parameters[1,16,18,44]. The main limitations include the difficulty to identify the exact limits of the lesion, the degree of malignancy and the differentiation between tumoral recurrence and radionecrosis[11,16]. Over recent decades, new complementary MRI techniques have been developed that supply quantitative parameters providing functional or metabolic-biochemical data[1,35,58]. Perfusion-weighted imaging (PWI), one of these techniques, has become a powerful tool in neuroradiology.

Perfusion-weighted imaging may be performed as a complementary examination to conventional MRI techniques, giving non-invasive access to brain hemodynamic parameters and demonstrating regional variations of microcirculation by mapping[15,48]. Cerebral perfusion is defined as the volume of blood that passes through a determined tissue mass over a unit of time[11,30]. In PWI, however, the term "perfusion" includes several hemodynamic measurements such as the cerebral blood volume (CBV), cerebral blood flow (CBF) and the mean transit time (MTT)[11,39,42,58].

The clinical applications of PWI in the evaluation of focal brain lesions include the differentiation between neoplastic and infectious lesions, primary tumors and solitary metastasis and, in the post-treatment follow up, the differentiation of tumoral recurrence and radionecrosis[9,15,26,29,42,59].

The goal of this article is to present a review about the role of perfusion-weighted MRI in the evaluation of solitary or multiple, neoplastic and infectious, focal brain lesions.

Technical considerations

Basically there are two MRI techniques for the evaluation of cerebral hemodynamics: dynamic susceptibility contrast-enhanced (DSC), achieved with a bolus injection of magnetic contrast agent (para- or superparamagnetic) that, on passing through the capillary network, determines transitory alterations in the magnetic field of the cerebral tissue measured by means of variations in the signal intensity, and the arterial spin labeling (ASL) technique which uses manipulation of the magnetization of the water molecules present in the blood to obtain an endogen marker of the blood flow[31,55].

The DSC MRI technique, first described by Rosen et al.[45] in 1991, uses rapid image sequence acquisition that can be T1 or T2-weighted, each one of which presents with specific advantages and disadvantages. The T2-weighted DSC technique uses spin-echo (SE) or gradient-echo (GRE) sequences, with the latter being denominated T2*. Spin-echo sequences have the advantage of diminishing artifacts at brain-bone and brain-air interfaces and is more sensitive to signal changes of the magnetic contrast agent passing through small vessels including capillaries. Its main disadvantage is the necessity of a larger dose of magnetic contrast agent to determine similar signal alterations when compared to GRE sequences. The T1-weighted DSC technique has the advantage of requiring a smaller dose of magnetic contrast agent and provides a better temporal resolution however its main disadvantage is that the extravasation of contrast due to blood-brain barrier (BBB) disruption may lead to errors in measurements of hemodynamic parameters[16,30,37,42,60]. The disruption of the BBB, frequently observed in malignant tumors, with consequent extravasation and recirculation of the contrast, is a limitation of the perfusion method due to the T1 shortening effect that causes an underestimation of the CBV[16]. There is thus, in these cases, the necessity to correct this effect so as not to underestimate the values of CBV[6]. One manner to reduce it is to utilize a gamma-variate function on the measured signal intensity versus time curve which provides the different parameters related to relative hemodynamics. However, this analysis does not give an absolute value of CBV, but provides a relative measurement; the relative CBV (rCBV) is proportional to the area under the corrected curve[9,11,16,30,34,35].

The main contraindication of techniques that employ paramagnetic gadolinium-based contrast agents, is their association with the development of nephrogenic systemic fibrosis in patients with advanced renal failure (glomerular filtration rates of less than 30 mL/min/1.73m^2), in particular dialysis patients[7,47].

Although DSC MRI is the technique most commonly employed in the clinical practice, the ASL technique has demonstrated promising results in clinical diagnosis. The production of perfusion images with ASL, contrary to the techniques that use exogen contrast agents, is totally non-invasive; its contrast agent is diffusible and has greater temporal resolution, reproducibility and measuring capacity. The limitations originate, mainly, from its low signal-to-noise ratio, accentuated sensitivity to movement artifacts and the long time needed for the acquisition of images, which have been the impetus for research and development of different resources in an attempt to improve and, consequently, widen the technique's clinical applicability[8,19,38,39,56,58].

Clinical applications

Conventional MRI with T1 and T2-weighted images is often utilized in the diagnosis of brain lesions with the evaluation of focal or diffused involvement, presence or absence of edema, hemorrhage, necrosis, increases in the intracranial pressure, mass effect and characterization of the pattern of contrast enhancement of the lesions, which may indirectly identify the degree of aggressiveness, even though there is controversy about the data obtained by this imaging method and the anatomopathological results[10,36,40,51].

According to Law et al.[36] the presence of a disruption of the BBB is frequently associated to malignant neoplasms, however contrast enhancement of the lesion does not demonstrate the degree of malignity. The perilesional hyperintensity on conventional T2-weighted MRI presents a low specificity, and may represent tumoral infiltration, vasogenic edema or both. In respect to the mass effect and the presence of necrosis, Dean et al.[17] stress that these parameters are the most important predictive factors of the degree of malignancy, however they are not specific[36].

The study of PWI can be utilized together with conventional MRI to demonstrate regional variations in the cerebral microcirculation by means of rCBV maps[15,48]. Relative cerebral blood volume maps show vascularization of brain lesions, which indirectly estimate angiogenesis, thereby identifying lesions that may be similar to neoplasms, to infectious or inflammatory processes, to tumefactive demyelinating lesions or to necrosis induced by radiation[9,21,46].

Perfusion-weighted MRI in focal neoplastic lesions

Gliomas are the most common primary tumors of the central nervous system (CNS), accounting for 40% of all primary intracranial neoplasms, with glioblastoma multiforme being the most common malignant subtype corresponding to 12 to 15% of all intracranial neoplasms[2,25]. Perfusion-weighted imaging studies of malignant gliomas show higher rCBV values (Figure 1) when compared to glial neoplasms with low degrees of anaplasia[26,43] (Figure 2).

Although several authors have demonstrated significant correlations between the rCBV and the degree of malignancy of glial tumors[12,18,29,53], the increase in the vascularization does not necessarily signify malignancy[11]. The best example is the oligodendroglioma, considered a non-astrocyte glial tumor that presents a high rCBV value (Figure 3) as, one characteristic of this tumor is its rich and delicate capillary network; histologically it is characterized with a low grade of malignancy[13,32].

Metastases are the most frequent intracranial tumors in adults and generally occur by hematogenous dissemination[11,20]. Solitary metastasis occur in 30 to 50% of the cases thus making differential diagnosis with primary tumors difficult, mainly when there is no information about the involvement outside the CNS[11,12].

Brain perfusion-weighted MRI is not capable of differentiating primary tumors from solitary metastasis as both lesions are hypervascularized and thus present high rCBV values. However, there is a difference in the rCBV measured in the perilesional region which presents a higher value in primary tumors compared to metastases. This may be explained by the fact that in metastasis there is only vasogenic edema in the perilesional region without histological evidence of tumor beyond the outer enhancing margin. On the other hand, with primary tumors, the perilesional region presents with vasogenic edema and tumoral cell infiltration in the perivascular spaces[1,9,11,12,33,57].

Primary lymphomas of the CNS have been increasing in incidence in immunocompetent and immunodepressed individuals, representing up to 16% of all primary brain tumors[11,50]. Lymphoma and toxoplasmosis are the most frequent focal brain lesions in acquired immunodeficiency syndrome patients and are difficult to differentiate by conventional MRI methods as they can be solitary or multiple and not infrequently exhibit peripheral enhancement by the contrast agent[22,50]. The role of PWI is to detect and quantify angiogenesis and so it is consequently useful to differentiate between lymphomas, toxoplasmosis and highly malignant gliomas, although angiogenesis is not a prominent characteristic of lymphomas. Several authors have demonstrated that the rCBV values of lymphomas are higher than those of toxoplasmosis infections and lower than those of highly malignant glial neoplasms[14,22,27,28,53,57].

Fig. 1

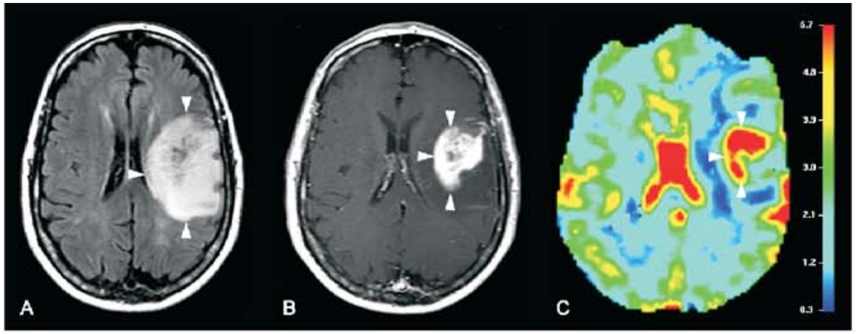

Fig. 2

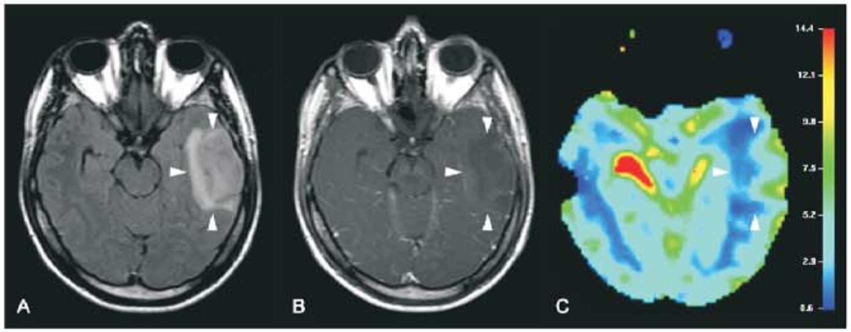

Fig. 3

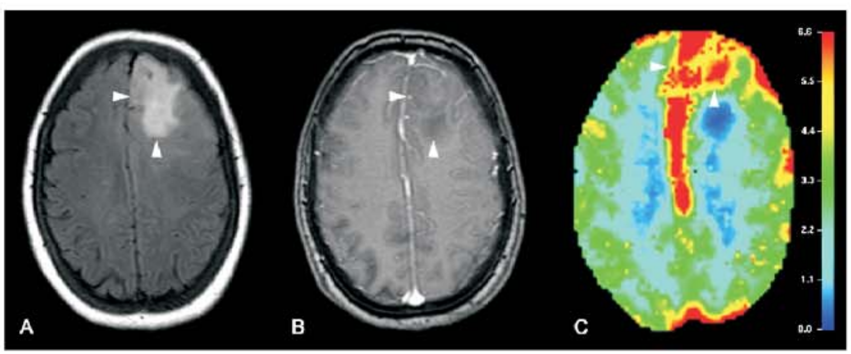

Fig. 4

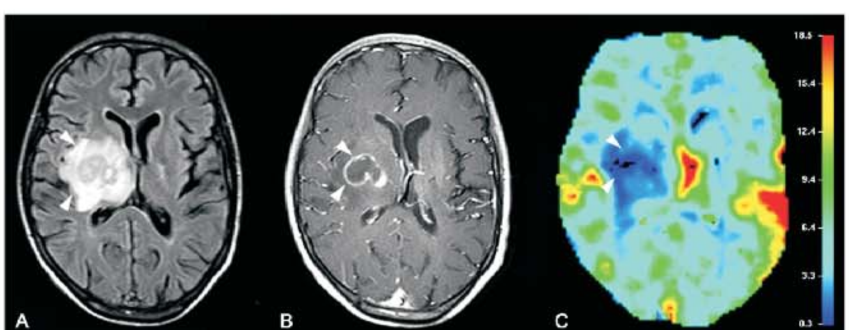

Fig. 5

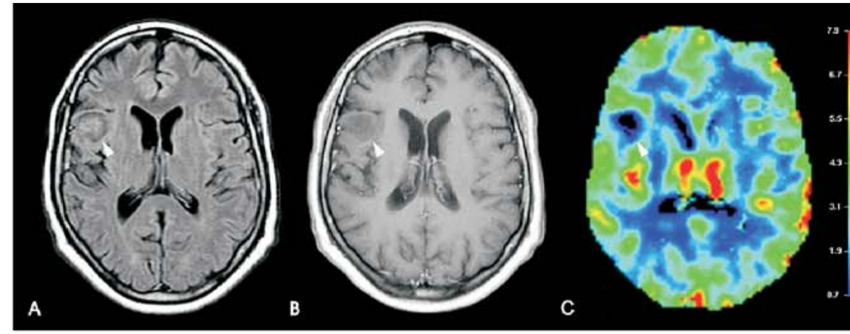

Fig. 6

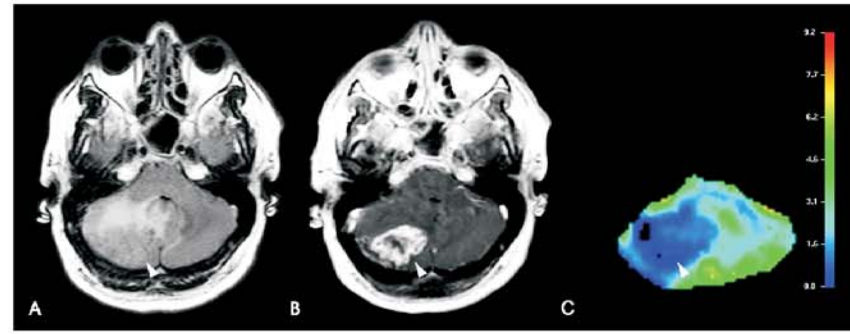

Fig. 7

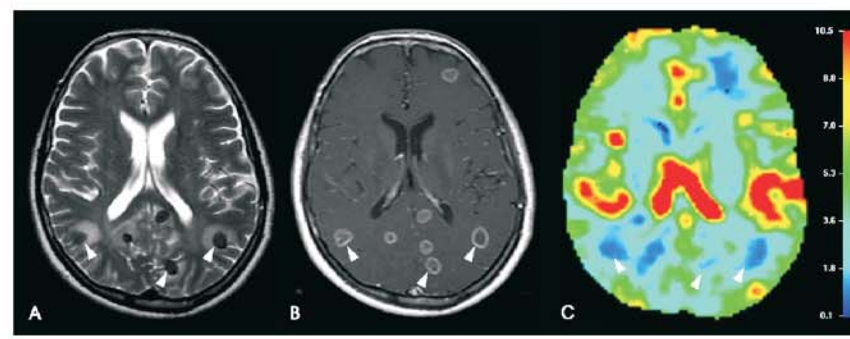

Fig. 8

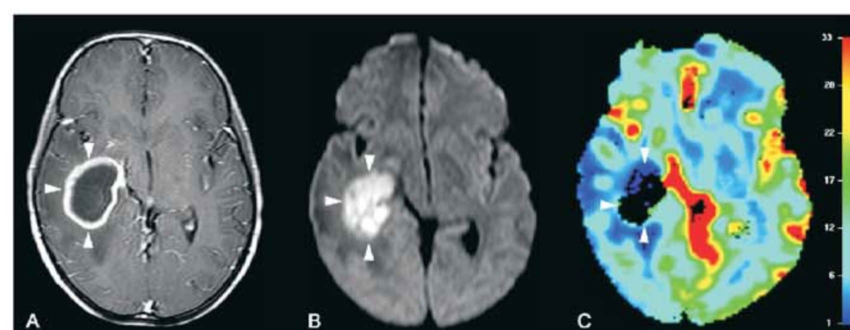

Figure 1. Glioblastoma multiforme in a 72-year-old man. (A) Axial fluid-attenuated inversion recovery (FLAIR) MR image showing a heterogeneous mass with moderate peritumoral edema in the left frontal lobe (arrowheads). (B) Axial contrast-enhanced T1-weighted MR image showing irregularly enhanced mass (arrowheads). (C) Axial rCBV color map demonstrating an area of hypervascularity (high rCBV value) in the tumor (arrowheads).

Figure 2. Low-grade fibrillary astrocytoma in a 23-year-old man. (A) Axial FLAIR MR image showing a hyperintense mass in the left temporal lobe (arrowheads). (B) Axial contrast-enhanced T1-weighted MR image showing a non-enhanced left temporal lobe tumor (arrowheads). (C) Axial rCBV color map demonstrating no evidence of increased vascularity (low rCBV value) in the tumor (arrowheads).

Figure 3. Oligodendroglioma in a 46-year-old woman. (A) Axial FLAIR MR image showing a hyperintense mass in the left frontal lobe (arrowheads). (B) Axial contrast-enhanced T1-weighted MR image showing a non-enhanced left frontal lobe tumor (arrowheads). (C) Axial rCBV color map demonstrating a focus of increased vascularity (high rCBV value) in the tumor (arrowheads).

Figure 4. Toxoplasmosis lesion in a 29-year-old man with AIDS. (A) Axial FLAIR MR image showing a hyperintense mass surrounded by edema in the right basal ganglia (arrowheads). (B) Axial contrast-enhanced T1-weighted MR image showing enhanced rim lesion (arrowheads). (C) Axial rCBV color map demonstrating no evidence of increased vascularity (low rCBV value) in the lesion (arrowheads).

Figure 5. Cysticercosis lesion in a 35-year-old man. (A) Axial FLAIR MR image showing an isointense mass without edema in the right frontal lobe (arrowhead). (B) Axial contrast-enhanced T1-weighted MR image showing a non-enhanced lesion (arrowhead). (C) Axial rCBV color map demonstrating no evidence of increased vascularity (low rCBV value) in the lesion (arrowhead). Follow-up confirmed neurocysticercosis.

Figure 6. Cryptococcosis lesion in a 48-year-old man. (A) Axial FLAIR MR image showing a hyperintense mass surrounded by edema in the right cerebellar hemisphere (arrowhead). (B) Axial contrast-enhanced T1-weighted MR image showing irregularly enhanced lesion (arrowhead). (C) Axial rCBV color map demonstrating no evidence of increased vascularity (low rCBV value) in the lesion (arrowhead). Surgical procedure and histopathology confirmed cryptococcoma in the immunocompetent patient.

Figure 7. Paracoccidioidomycosis lesions in a 45-year-old man. (A) Axial T2-weighted MR image showing hypointense lesions with hyperintense area of surrounding edema in both brain hemispheres (arrowheads). (B) Axial contrast-enhanced T1-weighted MR image showing the ring enhanced lesions (arrowheads). (C) Axial rCBV color map demonstrating no evidence of increased vascularity (low rCBV values) in the lesions (arrowheads).

Figure 8. Pyogenic abscess in a 10-year-old boy. (A) Axial contrast-enhanced T1-weighted MR image showing the ring enhanced lesion in the right temporal lobe (arrowheads). (B) Axial diffusion-weighted image demonstrating hyperintense necrotic center, which represents restricted diffusion (arrowheads). (C) Axial rCBV color map demonstrating no evidence of increased vascularity (low rCBV value) in the lesion (arrowheads).

Intracranial extra-axial neoplasms are highly vascularized tumors that originate in the meninges, ventricles, choroid plexus and pineal gland. Studies of extra-axial tumors using the perfusion technique show immediate and persistent extravasation of the contrast agent during dynamic imaging due to the absence of the BBB with consequent errors in the measurement of the rCBV[11].

Perfusion-weighted MRI is a useful tool to choose the site for stereotactic biopsies by characterization of the area with the greatest rCBV, which has demonstrated high correlation with anatomopathological results[4,11,16,41,53,59].

The differentiation between tumoral recurrence and radionecrosis can not be exactly ascertained by conventional MRI even with the utilization of a contrast agent and thus remains a challenge as the therapeutic conduct of these two entities is totally different. According to Covarrubias et al.[16] the damage of the BBB induced by radiotherapy determines the extravasation of the contrast agent to the interstice resulting in a lesion that can mimic tumoral recurrence. The evolutive control after treatment is frequently not useful, as radionecrosis generally occurs from six months to several years after radiotherapy, that is, the period during which recurrence is most probable. Additionally it is necessary to consider the possibility of coexistence of lesions.

Radionecrosis usually presents a low rCBV value, while in tumoral recurrence this value is high. Sugahara et al.[54] determined the value of perfusion-weighted MRI in the evaluation of intra-axial expansive processes after radiotherapeutic treatment and demonstrated that rCBV values greater than 2.6 were indicative of tumoral recurrence and rCBV values lower than 0.6 indicated radionecrosis.

Perfusion-weighted MRI in focal infectious lesions

Intra-axial infectious lesions present a variable aspect in PWI studies depending on the immunological status of the patient and the aggressiveness of the infectious agent[11].

In neurotoxoplasmosis lesions there is a reduction in the rCBV value measured at the lesion and the perilesional edema (Figure 4), with values below those of normal white matter[1]. This hypoperfusion is explained by vasoconstriction in the solid marginal portion of the lesion determined by an increase in the interstice pressure secondary to perilesional edema and by the reduction, or even absence, of vascularization inside the lesion[22]. Another parasitic infection of the central nervous system that usually has low values of rCBV is cysticercosis. Although considered the most common parasitic infection of the CNS, its diagnosis remains difficult. Magnetic resonance findings of cysticercosis are variable and depend on the stage of the evolution of the infection. According to Amaral et al.[3] the lack of hyperperfusion of the lesion makes the diagnosis of a neoplastic process is unlikely, thus implying a possible infectious cause (Figure 5).

In CNS tuberculosis, Batra & Tripathi[5] demonstrated that a significant number of lesions present high rCBV values, similar to those found with cerebral gliomas. However, the differentiation with primary CNS tumors can be achieved by means of the measurement of the perilesional rCBV, as lesions by infection present low rCBV values determined by vasoconstriction secondary to the increase in interstitial pressure caused by perilesional edema, while neoplasms present histological evidence of tumor beyond the outer enhancing margin and, consequently, high rCBV values. These authors stress, however, that it may be difficult to differentiate between tuberculoma and metastasis utilizing PWI alone, as both lesions present with low perilesional rCBV values.

Cryptococcosis is a common mycotic central nervous system infection caused by the fungus *Cryptococcus neoformans*. It is most frequently found as the pathological presentation of cryptococcal meningoencephalitis. Other rare forms of central nervous system cryptococcal infections are their solid-granulomatous appearance and abscesses, both being commonly named cryptococcomas, because of the mass effect they cause in surrounding tissue that often simulates a brain tumor[49]. The measurement of rCBV in these lesions demonstrates low values denoting an infectious cause (Figure 6).

Paracoccidioidomycosis (PCM) is the most common endemic systemic mycosis in Latin America, with Brazil accounting for 80% of the cases reported worldwide[23,52]. Involvement of the CNS can vary in between 9.9 and 27.3% of the cases[23]. Until now there are no studies about the role of PWI in the evaluation of intracranial granulomatous lesions secondary to PCM. In our service, we performed perfusion-weighted MRI in one patient with granulomatous neuroparacoccidioidomycosis, which demonstrated a reduction in the rCBV value (Figure 7). However, further studies with a larger sample size should be performed before arriving at any conclusion on the pattern of these lesions.

Cerebral abscesses, usually caused by a pyogenic bacterial organism, are characterized by a central area of cellular degradation with an accumulation of purulent exudate and a poorly vascularized capsule of collagen which causes a reduction in the rCBV[5,12,28] (Figure 8). However, there are descriptions of cases with increases in the rCBV in the capsular portion of the lesion that are enhanced after the administration of a contrast agent[15]. Holmes et al.[28] stressed that this discordance between the rCBV values found with abscesses may be explained by the measurement of only one arbitrary area of the lesion, while Ferreira et al.[24] highlighted that, in latter stages, the capsule of the abscess may present an increase in the rCBV.

The differentiation between cerebral abscesses and cystic or necrotic tumors can be attained utilizing rCBV maps. While the capsular portion of abscesses is hypovascularized causing a reduction in the rCBV, the peripheral portion of tumors is hypervascularized and, thus, presents an increase in the rCBV[14,21].

Other clinical applications of perfusion-weighted MRI

Perfusion-weighted imaging has been utilized for other clinical applications, such as, in the viability of tissue surrounding areas of acute cerebral ischemia (ischemic penumbra), evaluation of tumefactive demyelinating lesions, therapeutic response of patients submitted to anti-angiogenic drug therapy, characterization of other diseases including reversible posterior encephalopathy or hypertensive encephalopathy, dementia, epilepsy, migraine and the effect of psychoactive drugs such as cocaine, with many publications available in the literature[11,16,42,46].

References

1. Al-Okaili RN, Krejza J, Wang S, Woo JH, Melhem ER. Advanced MR imaging techniques in the diagnosis of intraaxial brain tumors in adults. Radiographics 2006;26(Suppl 1):S173-S189.

2. Altman DA, Atkinson DS, Brat DJ. Best cases from the AFIP: glioblastoma multiforme. Radiographics 2007;27:883-888.

3. Amaral LL, Ferreira RM, Rocha AJ, Ferreira NP. Neurocysticercosis: evaluation with advanced magnetic resonance techniques and atypical forms. Top Magn Reson Imaging 2005:16;127-144.

4. Aronen HJ, Gazit IE, Louis DN, et al. Cerebral blood volume maps of gliomas: comparison with tumor grade and histologic findings. Radiology 1994;191:41-51.

5. Batra A, Tripathi RP. Perfusion magnetic resonance imaging in intracerebral parenchymal tuberculosis: preliminary findings. J Comput Assist Tomogr 2003;27:882-888.

6. Boxerman JL, Schmainda KM, Weisskoff RM. Relative cerebral blood volume maps corrected for contrast agent extravasation significantly correlate with glioma tumor grade, whereas uncorrected maps do not. AJNR Am J Neuroradiol 2006;27:859-867.

7. Broome DR. Nephrogenic systemic fibrosis associated with gadolinium based contrast agents: a summary of the medical literature reporting. Eur J Radiol 2008;66:230-234.

8. Brown GG, Clark C, Liu TT. Measurement of cerebral perfusion with arterial spin labeling: Part 2. Applications. J Int Neuropsychol Soc 2007;13:526-538.

9. Bulakbasi N, Kocaoglu M, Farzaliyev A, Tayfun C, Ucoz T, Somuncu I. Assessment of diagnostic accuracy of perfusion MR imaging in primary and metastatic solitary malignant brain tumors. AJNR Am J Neuroradiol 2005;26:2187-2199.

10. Calli C, Kitis O, Yunten N, Yurtseven T, Islekel S, Akalin T. Perfusion and diffusion MR imaging in enhancing malignant cerebral tumors. Eur J Radiol 2006;58:394-403.

11. Cha S, Knopp EA, Johnson G, Wetzel SG, Litt AW, Zagzag D. Intracranial mass lesions: dynamic contrast-enhanced susceptibility-weighted echo-planar perfusion MR imaging. Radiology 2002; 223:11-29.

12. Cha S, Lupo JM, Chen MH, et al. Differentiation of glioblastoma multiforme and single brain metastasis by peak height and percentage of signal intensity recovery derived from dynamic susceptibility-weighted contrast-enhanced perfusion MR imaging. AJNR Am J Neuroradiol 2007;28:1078-1084.

13. Cha S, Tihan T, Crawford F, et al. Differentiation of low-grade oligodendrogliomas from low-grade astrocytomas by using quantitative blood-volume measurements derived from dynamic susceptibility contrast-enhanced MR imaging. AJNR Am J Neuroradiol 2005;26:266-273.

14. Chan JH, Tsui EY, Chau LF, et al. Discrimination of an infected brain tumor from a cerebral abscess by combined MR perfusion and diffusion imaging. Comput Med Imaging Graph 2002;26:19-23.

15. Cho SK, Na DG, Ryoo JW, et al. Perfusion MR imaging: clinical utility for the differential diagnosis of various brain tumors. Korean J Radiol 2002;3:171-179.

16. Covarrubias DJ, Rosen BR, Lev MH. Dynamic magnetic resonance perfusion imaging of brain tumors. Oncologist 2004;9:528-537.

17. Dean BL, Drayer BP, Bird CR, et al. Gliomas: classification with MR imaging. Radiology 1990;174:411-415.

18. Debnam JM, Ketonen L, Hamberg LM, Hunter GJ. Current techniques used for the radiologic assessment of intracranial neoplasms. Arch Patol Lab Med 2007;131:252-260.

19. Deibler AR, Pollock JM, Kraft RA, Tan H, Burdette JH, Maldjian JA. Arterial spin-labeling in routine clinical practice, part 1: technique and artifacts. AJNR Am J Neuroradiol 2008;29:1228-1234.

20. Eichler AF, Loeffler JS. Multidisciplinary management of brain metastases. Oncologist 2007;12:884-898.

21. Erdogan C, Hakyemez B, Yildirim N, Parlak M. Brain abscess and cystic brain tumor: discrimination with dynamic susceptibility contrast perfusion-weighted MRI. J Comput Assist Tomogr 2005; 29:663-667.

22. Ernst TM, Chang L, Witt MD, et al. Cerebral toxoplasmosis and lymphoma in AIDS: perfusion MR imaging experience in 13 patients. Radiology 1998;208:663-669.

23. Fagundes-Pereyra WJ, Carvalho GT, Góes AM, Chagas Lima e Silva F, Sousa AA. Central nervous system paracoccidioidomycosis: analysis of 13 cases. Arq Neuropsiquiatr. 2006;64:269-276.

24. Ferreira NP, Otta GM, Amaral LL, Rocha AJ. Imaging aspects of pyogenic infections of the central nervous system. Top Magn Reson Imaging 2005;16:145-154.

25. Grier JT, Batchelor T. Low-grade gliomas in adults. Oncologist 2006;11:681-693.

26. Hakyemez B, Erdogan C, Ercan I, Ergin N, Uysal S, Atahan S. High-grade and low-grade gliomas: differentiation by using perfusion MR imaging. Clin Radiol 2005;60:493-502.

27. Hartmann M, Heiland S, Harting I, et al. Distinguishing of primary cerebral lymphoma from high-grade glioma with perfusion-weighted magnetic resonance imaging. Neurosci Lett 2003;338:119-122.

28. Holmes TM, Petrella JR, Provenzale JM. Distinction between cerebral abscesses and high-grade neoplasms by dynamic susceptibility contrast perfusion MRI. AJR Am J Roentgenol 2004;183:1247-1252.

29. Hourani R, Brant LJ, Rizk T, Weingart JD, Barker PB, Horska A. Can proton MR spectroscopic and perfusion imaging differentiate between neoplastic and nonneoplastic brain lesions in adults? AJNR Am J Neuroradiol 2008;29:366-372.

30. Keston P, Murray AD, Jackson A. Cerebral perfusion imaging using contrast-enhanced MRI. Clin Radiol 2003;58:505-513.

31. Knutsson L, Bloch KM, Holtas S, Wirestam R, Stahlberg F. Model-free arterial spin labelling for cerebral blood flow quantification: introduction of regional arterial input functions identified by factor analysis. Magn Reson Imaging 2008;26:554-559.

32. Koeller KK, Rushing EJ. From the archives of the AFIP: Oligodendroglioma and its variants: radiologic-pathologic correlation. Radiographics 2005;25:1669-1688.

33. Law M, Cha S, Knopp EA, Johnson G, Arnett J, Litt AW. High-grade gliomas and solitary metastases: differentiation by using perfusion and proton spectroscopic MR imaging. Radiology 2002;222:715-721.

34. Law M, Oh S, Babb JS, et al. Low-grade gliomas: dynamic susceptibility-weighted contrast-enhanced perfusion MR imaging - prediction of patient clinical response. Radiology 2006;238:658-667.

35. Law M, Yang S, Babb JS, et al. Comparison of cerebral blood volume and vascular permeability from dynamic susceptibility contrast-enhanced perfusion MR imaging with glioma grade. AJNR Am J Neuroradiol 2004;25:746-755.

36. Law M, Yang S, Wang H, et al. Glioma grading: sensitivity, specificity, and predictive values of perfusion MR imaging and proton MR spectroscopic imaging compared with conventional MR imaging. AJNR Am J Neuroradiol 2003;24:1989-1998.

37. Le Bas JF, Grand S, Krainik A, Lefournier V, Tropres I, Rémy C. Perfusion MR imaging in brain tumors. J Radiol 2006;87:807-821.

38. Liu TT, Brown GG. Measurement of cerebral perfusion with arterial spin labeling: Part 1. Methods. J Int Neuropsychol Soc 2007;13:517-525.

39. Luypaert R, Boujraf S, Sourbron S, Osteaux M. Diffusion and perfusion MRI: basic physics. Eur J Radiol 2001;38:19-27.

40. Maia AC Jr, Malheiros SM, Rocha AJ, et al. MR cerebral blood volume maps correlated with vascular endothelial growth factor expression and tumor grade in nonenhancing gliomas. AJNR Am J Neuroradiol 2005;26:777-783.

41. Maia AC Jr, Malheiros SM, Rocha AJ, et al. Stereotactic biopsy guidance in adults with supratentorial nonenhancing gliomas: role of perfusion-weighted magnetic resonance imaging. J Neurosurg 2004;101:970-976.

42. Petrella JR, Provenzale JM. MR perfusion imaging of the brain: techniques and applications. AJR Am J Roentgenol 2000;175:207-219.

43. Preul C, Kuhn B, Lang EW, Mehdorn HM, Heller M, Link J. Differentiation of cerebral tumors using multi-section echo planar MR perfusion imaging. Eur J Radiol 2003;48:244-251.

44. Rollin N, Guyotat J, Streichenberger N, Honnorat J, Tran Minh VA, Cotton F. Clinical relevance of diffusion and perfusion magnetic resonance imaging in assessing intraaxial brain tumors. Neuroradiology 2006;48:150-159.

45. Rosen BR, Belliveau JW, Aronen HJ, et al. Susceptibility contrast imaging of cerebral blood volume: human experience. Magn Reson Med 1991;22:293-299.

46. Rowley HA, Roberts TPL. Clinical perspectives in perfusion: neuroradiologic applications. Top Magn Reson Imaging 2004;15:28-40.

47. Sadowski EA, Bennett LK, Chan MR, et al. Nephrogenic systemic fibrosis: risk factors and incidence estimation. Radiology 2007;243:148-157.

48. Schmainda KM, Rand SD, Joseph AM, et al. Characterization of a first-pass gradient-echo spin-echo method to predict brain tumor grade and angiogenesis. AJNR Am J Neuroradiol 2004;25:1524-1532.

49. Sillero-Filho VJ, Souza AB, Vaitsman RP, et al. Cerebellar cryptococcoma simulating metastatic neoplasm. Arq Neuropsiquiatr 2009;67:290-292.

50. Slone HW, Blake JJ, Shah R, Guttikonda S, Bourekas EC. CT and MRI findings of intracranial lymphoma. AJR Am J Roentgenol 2005;184:1679-1685.

51. Smirniotopoulos JG, Murphy FM, Rushing EJ, Rees JH, Schroeder JW. Patterns of contrast enhancement in the brain and meninges. Radiographics 2007; 27: 525-551.

52. Souza AS Jr, Gasparetto EL, Davaus T, Escuissato DL, Marchiori E. High-resolution CT findings of 77 patients with untreated pulmonary paracoccidioidomycosis. AJR Am J Roentgenol 2006;187:1248-1252.

53. Sugahara T, Korogi Y, Kochi M, et al. Correlation of MR imaging-determined cerebral blood volume maps with histologic and angiographic determination of vascularity of gliomas. AJR Am J Roentgenol 1998;171:1479-1486.

54. Sugahara T, Korogi Y, Tomiguchi S, et al. Posttherapeutic intraaxial brain tumor: the value of perfusion-sensitive contrast-enhanced MR imaging for differentiating tumor recurrence from nonneoplastic contrast-enhancing tissue. AJNR Am J Neuroradiol 2000;21:901-909.

55. van Laar PJ, van der Grond J, Hendrikse J. Brain perfusion territory imaging: methods and clinical applications of selective arterial spin-labeling MR imaging. Radiology 2008;246:354-364.

56. Warmuth C, Gunther M, Zimmer C. Quantification of blood flow in brain tumors: comparison of arterial spin labeling and dynamic susceptibility-weighted contrast-enhanced MR imaging. Radiology 2003;228:523-532.

57. Weber MA, Zoubaa S, Schlieter M, et al. Diagnostic performance of spectroscopic and perfusion MRI for distinction of brain tumors. Neurology 2006;66:1899-1906.

58. Wintermark M, Sesay M, Barbier E, et al. Comparative overview of brain perfusion imaging techniques. J Neuroradiol 2005;32:294-314.

59. Wong JC, Provenzale JM, Petrella JR. Perfusion MR imaging of brain neoplasms. AJR Am J Roentgenol 2000;174:1147-1157.

60. Wu O, Ostergaard L, Sorensen AG. Technical aspects of perfusion-weighted imaging. Neuroimag Clin N Am 2005;15:623-637.